Plasma proteomics identifies leukemia inhibitory factor (LIF) as a novel predictive biomarker of immune-checkpoint blockade resistance

Y. Loriot, A. Marabelle, J.P. Guégan, F.X. Danlos, B. Besse, N. Chaput, C. Massard, D. Planchard, C. Robert, C. Even, et al.

ORIGINAL ARTICLE

Plasma proteomics identifies Leukemia Inhibitory Factor (LIF) as a novel predictive biomarker of immune-checkpoint blockade resistance

Y. Loriot[1*]; A. Marabelle[2*]; JP. Guégan[3] ; FX. Danlos[2] ; B. Besse[1,4] ; N. Chaput[5,6,7] ; C. Massard[2] ; D. Planchard[1] ; C. Robert[1] ; C. Even[1] ; M. Khettab[1] ; L. Tselika[8] ; L. Friboulet[9] ; F. André[14] ; I. Nafia[3] ; F. Le Loarer[10,11] ; JC Soria[1] ; A. Bessede[3¥] ; A. Italiano[¥2,11,12].

** Y.L. and A.M. contributed equally to this work*

[¥] A.B. and A.I. contributed equally to this work

1 Cancer Medicine Department, INSERM U981, Gustave Roussy, Université Paris-Saclay, F-94800 Villejuif, France.
2 Département d'Innovation Précoce et d'Essais Thérapeutiques (DITEP), INSERM U1015 & CIC1428, Université Paris Saclay, Gustave Roussy, Villejuif, France
3 Explicyte, 229 cours de l'Argonne, 33000 Bordeaux, France
4 Faculty of Medicine, University Paris-Saclay, F-94276 Le Kremlin Bicêtre, France.
5 Laboratory of Immunomonitoring in Oncology, Gustave Roussy Cancer Campus, CNRS-UMS 3655 and INSERM-US23, F-94805 Villejuif, France.
6 Faculty of Pharmacy, University Paris-Saclay, F-92296 Chatenay-Malabry, France.
7 Laboratory of Genetic Instability and Oncogenesis, UMR CNRS 8200, Gustave Roussy, Université Paris-Saclay, F-94805 Villejuif, France.
8 Interventional Radiology, Gustave Roussy, 94800 Villejuif
9 Université Paris-Saclay, Institut Gustave Roussy, Inserm U981, Biomarqueurs prédictifs et nouvelles stratégies thérapeutiques en oncologie, 94800 Villejuif, France
10 Department of Pathology, Institut Bergonié, Bordeaux, France
11 Faculty of Medicine, University of Bordeaux, Bordeaux, France
12 Department of Medicine, Institut Bergonié, Bordeaux, France

Correspondence to: Pr Antoine ITALIANO, Gustave Roussy, Rue Camille Desmoulins, Villejuif, France

Tel : +33 01 42 11 42 11

Email: antoine.italiano@gustaveroussy.fr

ABSTRACT

Background: Immune checkpoint blockers (ICBs) are now widely used in oncology. However, most patients do not derive benefit from these agents. Therefore, there is a crucial need to identify novel and reliable biomarkers of resistance to such treatments in order to prescribe potentially toxic and costly treatments only to patients with expected therapeutic benefits. In the wake of genomics, the study of proteins is now emerging as the new frontier for understanding real-time human biology.

Methods: We analyzed the proteome of plasma samples, collected before treatment onset, from two independent prospective cohorts of cancer patients treated with ICB (Discovery cohort n= 95, validation cohort n= 292). We then investigated the correlation between protein plasma levels, clinical benefit rate, progression-free survival (PFS) and overall survival (OS) by Cox proportional hazards models.

Results: By using an unbiased proteomics approach, we show that, in both Discovery and Validation cohorts, elevated baseline serum level of Leukemia Inhibitory Factor (LIF) is associated with a poor clinical outcome in cancer patients treated with ICB, independently of other prognostic factors. We also demonstrated that circulating level of LIF is inversely correlated with the presence of Tertiary Lymphoid Structures (TLS) in the tumor microenvironment.

Conclusion: This novel clinical dataset brings strong evidence for the role of LIF as a potential suppressor of anti-tumor immunity and suggest that targeting LIF or its pathway may represent a promising approach to improve efficacy of cancer immunotherapy in combination with ICB.

KEY WORDS: LIF, immunotherapy, biomarkers, resistance

HIGHLIGHTS

- Plasma proteomics identified Leukemia Inhibitory Factor (LIF) as a robust biomarker associated with resistance to immunotherapy
- Plasma levels of LIF are associated with tumor microenvironment features such as the presence of tertiary lymphoid structures
- LIF appears as an important therapeutic target to improve ICB efficacy

INTRODUCTION

The discovery of immune inhibitory checkpoints has revolutionized the systemic approach of the treatment of cancer. Blocking the interaction between the Programmed cell death 1 (PD-1) receptor and its primary ligand Programmed death-ligand 1 (PD-L1) has demonstrated remarkable anti-cancer activity and has led to the recent approval of anti-PD-1/PD-L1 drugs in several solid tumors[1]. However, most patients receiving anti-PD-1/PD-L1 monoclonal antibodies do not derive clinical benefit. Therefore, there is a crucial need to identify reliable predictive biomarkers of response to anti-PD-1/PD-L1 agents, both to develop precision medicine in cancer immunotherapy and to better understand mechanisms of sensitivity and resistance.

PD-L1 expression status as assessed by immunohistochemistry, tumor mutational burden and microsatellite instability status are so far the sole companion diagnostic markers approved to guide for anti-PD(L)1 therapy[2-4]. However, all of them and particularly PD-L1 expression are imperfect predictors of response to immune-checkpoint inhibition as demonstrated by the discordant results reported by multiple studies[2].

While tumor tissue profiling is important for biomarker discovery, this approach has several limitations including limited accessibility and temporal and spatial heterogeneity. Hence, identification of biomarkers than can be readily evaluable through peripheral blood sampling is crucial to allow the easiest implementation in routine clinical practice. To the best of our knowledge, we report here the first large analysis, including discovery and validation cohorts, of plasma proteome from cancer patients treated with immune checkpoint blockers (ICB).

METHODS

Patients (Figure 1)

This study was based on the analysis of two prospective cohorts of advanced cancer patients treated with ICB at Gustave Roussy (Villejuif, France) (Discovery: MATCH-R[5], NCT02517892; Validation cohort: PREMIS, NCT03984318). The inclusion criteria were age ≥ 18 years, histologically proven malignant tumor, unresectable and/or metastatic disease, at least one tumor evaluation by imaging after immunotherapy onset, and, for the MATCH-R study, availability of paraffin-embedded tumor material obtained before immunotherapy onset. Patients treated with combinations of ICB and chemotherapy were excluded from the analysis. Institutional ethics review board approval and patient informed consents were obtained for both studies.

Treatments and evaluation

All patients were treated either with anti-PD(L)1 monotherapies or anti-PD(L)1 based combination therapies. Patients were treated by immunotherapy either within clinical trials, or in the context of EMA-approved indications, or within early access programs. The best response to treatment was evaluated according to Response Evaluation Criteria in Solid Tumors (RECIST)[6] or iRECIST depending on the protocol in which patients were treated. Routine follow-up and treatment beyond progression therapeutic options were similar within the two cohorts. Durable clinical benefit (DCB) was defined as the proportion of patients achieving objective response or stable disease lasting ≥ 12 months. Progression-free survival (PFS) was defined as the time from the start of treatment until disease progression, death, or last patient contact. Overall survival (OS) was defined as the time from the start of treatment until death or last patient contact.

Plasma proteome analysis

Proteome analysis has been performed as previously described[7] thanks to the Olink Proximity Extension Assay (PEA) (Olink Proteomics AB, Uppsala, Sweden). In brief, pairs of oligonucleotide-labeled antibody probes bind to their targeted protein, and if the two probes are brought in proximity the oligonucleotides will hybridize in a pair-wise manner. The addition of a DNA polymerase leads to a proximity-dependent DNA polymerization event, generating a unique target sequence analyzed through either Next Generation Sequencing or Real-Time PCR.

Analysis of baseline samples from the discovery cohort has been performed using the Olink® Explore 1536 library consisting of 1472 proteins and 48 controls assays divided into four 384-plex panels focused on inflammation, oncology, cardiometabolic and neurology proteins. Sequencing was performed on a NovaSeq 6000 system using two S1 flow cells with 2 × 50 base read lengths. Counts of known sequences are thereafter translated into normalized protein expression (NPX) units through a QC and normalization process developed and provided by Olink.

Plasma samples from the validation cohort were assessed using the Olink® Target 96 Inflammation panel (Olink Proteomics AB, Uppsala, Sweden) according to the manufacturer's instructions[8]. In that case, the resulting DNA sequence was subsequently detected and quantified using a microfluidic real-time PCR instrument (Biomark HD, Fluidigm).

Data were quality controlled and normalized using an internal extension control and an inter-plate control, to adjust for intra- and inter-run variation. The final assay read-out is presented in Normalized Protein eXpression (NPX) values, which is an arbitrary unit on a log2-scale where a high value corresponds to a higher protein

expression. All assay validation data (detection limits, intra- and inter-assay precision data, etc.) are available on manufacturer's website (www.olink.com).

Immunohistochemistry stainings

All staining were carried out on 3,5 micrometers paraffin slides using a Ventana Discovery Ultra platform (Ventana, Roche Diagnostics). Double immunohistochemistry was performed on all cases with **i)** CD3 (2GV6, Ventana) combined with CD20 (L26, Ventana) and **ii)** CD8 (C8/144B, Dako) combined to PD-L1 (QR1, Diagomics). Stainings were performed with the protocol RUO discovery universal according to the manufacturer's recommendations with the detection kits OmniMap anti-Rb HRP (760-4311, Ventana) and OmniMap anti-Ms HRP (760-4310, Ventana).

Tumor TLS assessment

All cases were reviewed blindly by a pathologist for the presence of TLS according to the hematoxylin eosin saffron (HES) and the multiplexed immunohistochemistry on serial sections as previously described[9]. TLS were defined as lymphoid aggregates of B lymphocytes (admixed with a variable proportion of plasma cells and T lymphocytes in most cases). Only TLS made up of more than 50 cells and located either among the tumor cells or at the invasive margin (defined as fibrous tissue distant of less than 1mm from tumor cells) were considered. When the TLS status was assessed on lymphoid organs (namely lymph nodes, spleen, tonsils), TLS were only taken into account when admixed to tumor cells and if distant from the residual parenchyma, to exclude pre-existing lymphoid follicles.

Tumor PD-L1 scoring

For all tumors, the PD-L1 status was determined with TPS (tumor positive score) following guidelines. Only viable tumor cells displaying partial or complete staining for PD-L1 membrane expression were considered relative to the total number of tumor cells. Positive immune cells and neoplastic cells showing only cytoplasmic staining were excluded[10].

Semi-automated and quantitative analysis of T-cell infiltrate

Density of CD8+ T cells within the tumor lesion was obtained by image analysis after slides digitization on a multispectral slide-imaging platform (Vectra Polaris, Akoya Bioscience). Using Inform software (Akoya Bioscience, version 2.4.1), tissue segmentation and cell phenotyping were performed and allowed for CD8+ T cells detection within the tumor lesion previously annotated by an expert pathologist. Combining CD8+ T cell detection and calculation of the tumor lesion surface, density of CD8+ lymphocytes was obtained for each sample.

RNAseq analysis

RNA sequencing was performed as previously described[11]. Reads were aligned to the hg38 human genome assembly using Rsubread (version 2.2.6) without prior trimming[12]. Counts were then summarized at the gene level using FeatureCounts and normalized using Deseq2. Relative abundance of immune cell types was estimated using the ConcensusTME[13] on the CIBERSORT[14] and Bindea[15] gene sets.

Statistical analysis

The cutoff date for statistical analysis of baseline demographic data and clinical outcome was 11/30/2020. Descriptive statistics were used to describe the

distribution of variables in the population. Survival rates were estimated using the Kaplan–Meier method. Differences between groups were evaluated by chi-square test or Fisher's exact test for categorical variables and Student's test for continuous variables. Receiver operating characteristic (ROC) curve analysis was performed using the ROCit R package. Prognostic factors were planned to be identified by univariate and multivariate analyses using a Cox regression model. Variables tested in univariate analysis included age, gender, tumor type, number of metastatic sites, presence of liver metastasis, performance status (PS), number of previous lines of treatment, and LIF plasma levels. Variables associated with PFS and OS with a *P*-value <0.05 in the univariate analysis were planned to be included in the multivariate analysis. Analyses were carried out using SPSS 20.0 statistical software (IPSS Inc., Chicago, IL). All statistical tests were two-sided, and $P < 0.05$ indicated statistical significance.

RESULTS

Unbiased proteomic analysis identifies baseline serum level of Leukemia Inhibitory Factor (LIF) is associated with poor clinical outcome in cancer patients treated with immune-checkpoint blockers

To detect potential peripheral biomarkers of efficacy of ICB, we implemented a proteomics analysis based on the Proximity Extension Assay (PEA) technology and the use of Olink® Explore 1536 panel[7] (1472 proteins and 48 controls) on plasma samples, collected before anti-PD(L)1-based immunotherapy onset, from 95 patients enrolled prospectively in the MATCH-R study (NCT02517892, Discovery cohort) - patient's characteristics are described in Table 1. Proteomic analysis allowed for the detection and quantification of 1463 unique proteins in all plasma samples. We then explored the correlation for each marker –classified as High and Low according to their respective median value - with progression-free survival. Among several cytokines (Supplementary Figure 2) already known to be associated with clinical outcome in cancer patients treated with immunotherapy such as IL6, CXCL8 (IL8) or CXCL1 (**Supp. Fig.2**)[16-17], Leukemia Inhibitory Factor (LIF) was the most significantly associated with outcome (**Fig. 2a**). The median follow-up was 26.4 months. The median PFS of LIF^{Low} patients was 7.4 months (95% CI, 2.9–11.9) versus 1.7 months (95% CI, 1.3–2.1) in the LIF^{High} group, p<0.0001 (**Fig. 2b**). The 6-month, 1-year, and 2-year PFS rates were 55.9%, 41.5%, and 16.2% in LIF^{Low} group and 17%, 6.4% and 0% in the LIF^{High} group, respectively. At the time of analysis, 69 patients (72.6%) had died and 26 (27.4%) were still alive. The median overall survival (OS) was 21.7 months (95% CI, 12–31.4) in the LIF^{Low} group versus 4.3 months (95% CI, 3.4–5.1) in the LIF^{High} group, p<0.0001 (**Fig. 2b**). The 6-month, 1-year, and 2-year OS rates were 81.1%, 67.8%, and 47.2% in the LIF^{Low} group and 40.4%, 29%, and 10.6% in

the LIF^{High} group, respectively. Overall, LIF plasma levels were significantly lower in patients with durable clinical benefit in comparison with other patients (**Fig. 2c**). Indeed, in patients classified as plasma LIF^{High}, the durable clinical benefit rate was 6.4% versus 41.7% in LIF^{Low} patients (NPX value below the median), p<0.0001 (**Fig. 2d**). Also, to analyze the performance of baseline LIF level to predict the clinical benefit, we performed a univariate time-dependent ROC (Receiver Operating Characteristics) curve analysis and found an AUC (Area Under Curve) at 0,735 thus confirming its strong predictive value (**Supp. Fig. 1**).

Leukemia Inhibitory Factor (LIF) predicts outcome in cancer patients treated with immune-checkpoint blockers independently of PD-L1 expression status

We then performed an exploratory analysis investigating association of LIF level with clinical outcome according to PD-L1 expression score (**Fig. 3a**) and CD8+ T-cell infiltration density (**Fig. 3d**) - as assessed by multiplexed immunohistochemistry - in a sub-cohort of 59 patients with available matched-tumor tissue. The PD-L1 tumor proportion score (TPS) was ≥ 1% in 20 patients (33.9%) and < 1% in 39 patients (66,1%). Peripheral level of LIF was similar in patients with PD-L1-positive and negative tumors (**Fig. 3b**). The proportion of PD-L1-positive tumors was similar among tumors with a high level (46.1%) and a low level of circulating LIF (55%) (data not shown). Regardless of the PD-L1 expression status, and despite the limited size of the sub-cohort, we observed that patients with tumors characterized by a low level of circulating LIF had better outcome. Indeed, among patients with a PD-L1 TPS < 1%, the median PFS was 7 months (95% CI, 2.8–11.1) in the LIF^{Low} group versus 1.5 months (95% CI, 0.9–2) in the LIF^{High} group; overall log–rank test p=0.001 (PFS). Among patients with a PD-L1 TPS ≥ 1%, the median PFS was 6.3 months (95% CI,

0–13.5) in the LIF^{Low} group versus 2.2 months (95% CI, 0.6–3.7) in the LIF^{High} group, overall log–rank test p=0.106 (PFS) (**Fig. 3c**).

We then quantified the density of CD8+ T cells within the tumor lesion and considered highly infiltrated tumor when density was above the threshold value of 262.7/mm² (corresponding to the 75th percentile). Interestingly, CD8-infiltrated tumors were characterized by a lower level of peripheral LIF (**Fig. 3e**, p=0,02). Also, whatever the CD8 infiltration density of the tumor, circulating LIF level was significantly associated with an improved PFS in the low CD8+ T-cell density group (p=0,016), and a trend was observed in the high CD8+ T-cell density subgroup (p=0,062) (**Fig. 3f**). The lack of statistical significance in the high CD8+ T-cell density subgroup may be related to the low sample size.

Leukemia Inhibitory Factor (LIF) serum levels are associated with specific tumor microenvironment features and the presence of tertiary lymphoid structures

We then investigated whether circulating LIF level was correlated with the intratumor immune landscape through RNAseq expression data deconvolution with Bindea (**Fig. 4a**) or CIBERSORT (**Supp. Fig.3)** algorithms. A significant inverse correlation between LIF and B cells (**Fig. 4a and b**) as well as with follicular helper T cells (**Fig. 4a**) was observed. These two cell types are major components of the so called tertiary lymphoid structures (TLS)[17], and we therefore decided to assess the presence of TLS in tumor samples by using multiplexed-immunohistochemistry (**Fig. 4c**) as previously described[9]. We observed the presence of TLS in 22 cases (37.3%). The proportion of TLS positive cases was significantly higher in the LIF^{Low} group than in the LIF^{High} group; 50% vs 24.1%, p=0.04 (**Fig. 4d**).

Baseline serum levels of LIF predict outcome independently of other prognostic factors in a validation cohort of cancer patients treated with immune-checkpoint blockers

To confirm the robustness of the predictive value of peripheral LIF level, plasma samples collected from 292 patients enrolled in the PREMIS study (NCT03984318) – serving as a validation cohort – cytokines, including LIF, were measured using the Olink Target 96 inflammation panel. This assay relies on a qPCR readout which was found to be highly similar and correlated with the Olink® Explore 1536 panel[18]. We found improved objective response rate (32.2% vs 16.4%, p=0.002), durable clinical benefit rate (34.2% vs 17.8%, p=0.001) (**Fig. 5c**), PFS (5.1 vs 2.6 months, p<0.0001) (**Fig. 5a**), and OS (not reached vs 8.5 months, p<0.001) (**Fig. 5b**), in the LIF^{Low} group compared with the LIF^{High} group. AUC of the ROC curve analysis was evaluated at 0.622 (**Supp. Fig. 4**) thus confirming the predictive value of LIF in an independent validation cohort. On multivariate analysis, LIF plasma levels remained independently associated with both PFS and OS (table 2).

To confirm that our results were representative of all cancer types, we performed one additional analysis by stratifying patients included in the PREMIS study according to tumor type: non-small-cell lung cancer (NSCLC) or non- NSCLC cases. We observed in each stratum significantly higher objective response rate, durable clinical benefit rate, PFS and OS indicating that the predictive value of circulating LIF level was not solely driven by the NSCLC histology (**Supp. Fig. 5a and 5b)**

DISCUSSION

In the wake of genomics, the study of proteins is now emerging as the new frontier for understanding real-time human biology. Protein biomarker discovery enables identification of signatures with pathophysiological importance, bridging the gap between genomes and phenotypes. This type of data may have a deep impact on improving future healthcare, particularly with respect to precision medicine, but progress has been hampered by the lack of technologies that can provide reliable specificity, high throughput, good precision, and high sensitivity. Here, we used a Proximity Extension Assay (PEA) technology, a unique method where each biomarker is addressed by a matched pair of antibodies, coupled to unique, partially complementary oligonucleotides, and measured by next generation sequencing[7]. This enables a high level of multiplexing while maintaining high-level data quality. To the best of our knowledge, we report here the largest study implementing a comprehensive analysis of the plasma proteome to identify predictive biomarker of efficacy in cancer patients treated with ICB. In comparison with traditional biomarkers such as PD-L1 expression status, circulating biomarkers offer a promising alternative to address the pitfalls associated with analysis of tumor tissue such as temporal and spatial tumor heterogeneity.

Thanks to a robust methodology, we were able to identify, starting from a Discovery cohort, LIF as a predictive factor of objective response rate, PFS and OS in cancer patients treated with ICB. To strengthen this finding, these results have been validated using samples from an independent and large validation cohort. In addition, analysis of the lung adenocarcinoma cohort of the TCGA database (Broad GDAC 1/28/2016) demonstrated that LIF was not associated with prognosis of lung cancer

patients thus highlighting its specific predictive value for patients treated with anti-PD(L)1-based ICB (data not shown).

LIF is a pleiotropic cytokine involved in many physiological and pathological processes (reviewed in ref 19) and is highly expressed in a subset of tumors across multiple tumor types where it has been shown to be associated with poor prognosis. As recently shown by single-cell studies, LIF is mainly expressed by tumor cells[20]. However, the mechanisms involving this cytokine in cancer progression are not well understood. One of the first demonstration of the role of LIF in immunity was reported by Gao et al showing that LIF promotes self-tolerance by stimulating the Treg differentiation and inhibiting T helper type 17 cell differentiation[21]. Moreover, LIF favors the acquisition of an M2 phenotype by macrophages and the recruitment of myeloid-derived suppressor cells into the tumor microenvironment [22-23], all these mechanisms participating in the anti-tumor immune evasion. LIF has also been shown to regulate the maturation of dendritic cells (DCs), leading to the development of tolerogenic DCs, which contribute to an immunosuppressive microenvironment[24]. Interestingly, LIF neutralization was associated with strong inhibition of tumor growth in several preclinical models[25,26]. A recent study has also shown that LIF blockade is associated with an increased production of CXCL9 by macrophages and a concomitant decrease in CD206, CD163 and CCL2[26]. In our study, while baseline plasma LIF was associated with an intratumoral expression of LIF, no correlation was found for either CCL2, CD206 or CXCL9 (**Supp. Fig. 6**) – the same results were observed by analyzing *LIF* gene expression in tumor samples (*data not shown*). In addition, we highlighted that plasma LIF was positively associated with circulating IL6 and CCL2 (**Supp. Fig. 7**).

We therefore assessed whether the peripheral level of LIF was associated with specific tumor microenvironment features. By using both transcriptomic and multiplexed-IHC analysis, we found that low levels of LIF were strongly associated with the presence of follicular helper T (Tfh) and B cells in the context of TLS. TLS can be likened to micro-secondary lymphoid organs. TLS have been identified in several solid tumor types and are associated with better survival when present in the tumor microenvironment[27-30]. Higher densities of TLS were associated with an increased density of tumor-infiltrating CD8+ T lymphocytes[31-32] and with an activated and cytotoxic immune signature[30]. We have recently reported that the presence of TLS is highly predictive of improved outcomes in cancer patients treated with immune checkpoint inhibitors[11]. Preclinical data have suggested that LIF blockade promotes $CD8^+$ T cell infiltration in several tumors models[26]. In our study, we bring, for the first time, evidence suggesting that low level of LIF is associated with the presence of TLS, which could in turn favor antitumor T-cell immunity induction. The combination of anti-LIF and anti-PD1 antibodies has also been shown to be synergistic in pre-clinical tumor models[26].

Recently, the results of a phase I study investigating the safety and efficacy of MSC-1, a first-in-class humanized IgG1 monoclonal antibody that potently and selectively inhibits LIF, have been reported[33]. Eligible patients had advanced relapsed/refractory solid tumors and received treatment with MSC-1 intravenously (75mg-1500 mg) once every 3-weeks as a single agent until disease progression. Single agent MSC-1 was well tolerated with no dose limiting toxicities observed during the first cycle of treatment. Preliminary signs of activity were observed with disease stabilization in 9 patients out of 41. Interestingly, analysis of paired biopsies (before treatment onset and on treatment) showed increase CD8 T-cell infiltration in a subset of samples.

Our results indicate that LIF could represent a key factor in resistance to cancer immunotherapy and thus suggest that targeting LIF axis may represent a promising approach to improve efficacy of ICB in cancer patients, and particularly in patients characterized by a high plasma level of LIF.

AUTHOR CONTRIBUTIONS

AI, AB, conceived and designed the study. FLL performed the histological analyses. YL, AM, FXD, BB, NC, CM, DP, CR, CE, MK, LT, LF, FA, JCS provided study material or treated patients. All authors collected and assembled data. AI, and AB developed the tables and figures. AI and AB conducted the literature search and wrote the manuscript. All authors were involved in the critical review of the manuscript and approved the final version.

FUNDING STATEMENT

None

DECLARATION OF INTERESTS

CM, FXD, MK, LT, LF, FLL, FA: Nothing to disclose

AB and JPG: Employees of Explicyte

AI: Received research grants from Astra Zeneca, Bayer, BMS, Chugai, Merck, MSD, Pharmamar, Novartis, Roche, and received personal fees from Epizyme, Bayer, Lilly, Roche, and Springworks

BB: Received grants from AstraZeneca , Pfizer , Eli Lilly , Onxeo , Bristol Myers Squibb, Inivata , Abbvie , Amgen , Blueprint Medicines , Celgene , GlaxoSmithKline , Ignyta , Ipsen , Merck KGaA , MSD Oncology , Nektar , PharmaMar , Sanofi , Spectrum Pharmaceuticals , Takeda , Tiziana Therapeutics , Cristal Therapeutics , Daiichi Sankyo , Janssen Oncology , OSE Immunotherapeutics , BeiGene , Boehringer Ingelheim , Genentech , SERVIER , Tolero Pharmaceuticals

YL: Received grants and personal fees from Janssen, during the conduct of the study; personal fees and non-financial support from Astellas, grants and personal fees from Sanofi, personal fees and non-financial support from Roche, personal fees and non-financial support from AstraZeneca, grants, personal fees and non-financial support from MSD, personal fees and non-financial support from BMS, personal fees from Clovis , personal fees and non-financial support from Seattle Genetics, personal fees from Incyte, personal fees from Pfizer.

AM: Received research grants from Mersu, Bristol-Myers Squibb, Boehringer Ingelheim, Transgene, MSD and received personal fees from Bristol-Myers Squibb, AstraZeneca, MedImmune, Oncovir, Merieux

JCS: Has received consultancy fees from AstraZeneca, Astex, Clovis, GSK, GamaMabs, Lilly, MSD, Mission Therapeutics, Merus, Pfizer, Pharma Mar, Pierre Fabre, Roche/Genentech, Sanofi, Servier, Symphogen, and Takeda.

All remaining authors have declared no conflicts of interest.

DATA SHARING STATEMENT

Individual participant data that underlie the results reported in this article will be available after deidentification beginning 24 months and ending 48 months following article publication to researchers who provide a methodologically sound proposal. Requests should be sent to the corresponding author.

REFERENCES

1. Vaddepally RK, Kharel P, Pandey R, Garje R, Chandra AB. Review of Indications of FDA-Approved Immune Checkpoint Inhibitors per NCCN Guidelines with the Level of Evidence. Cancers (Basel). 2020 Mar 20;12(3).
2. Davis AA, Patel VG. The role of PD-L1 expression as a predictive biomarker: an analysis of all US Food and Drug Administration (FDA) approvals of immune checkpoint inhibitors. J Immunother Cancer. 2019;7(1):278.
3. Marabelle A, Fakih M, Lopez J, Shah M, Shapira-Frommer R, Nakagawa K, Chung HC, Kindler HL, Lopez-Martin JA, Miller WH Jr, Italiano A, Kao S, Piha-Paul SA, Delord JP, McWilliams RR, Fabrizio DA, Aurora-Garg D, Xu L, Jin F, Norwood K, Bang YJ. Association of tumour mutational burden with outcomes in patients with advanced solid tumours treated with pembrolizumab: prospective biomarker analysis of the multicohort, open-label, phase 2 KEYNOTE-158 study. Lancet Oncol. 2020 Oct;21(10):1353-1365.
4. André T, Shiu KK, Kim TW, Jensen BV, Jensen LH, Punt C, Smith D, Garcia-Carbonero R, Benavides M, Gibbs P, de la Fouchardiere C, Rivera F, Elez E, Bendell J, Le DT, Yoshino T, Van Cutsem E, Yang P, Farooqui MZH, Marinello P, Diaz LA Jr; KEYNOTE-177 Investigators. Pembrolizumab in Microsatellite-Instability-High Advanced Colorectal Cancer. N Engl J Med. 2020 Dec 3;383(23):2207-2218.
5. Recondo G, Mahjoubi L, Maillard A, Loriot Y, Bigot L, Facchinetti F, Bahleda R, Gazzah A, Hollebecque A, Mezquita L, Planchard D, Naltet C, Lavaud P, Lacroix L, Richon C, Lovergne AA, De Baere T, Tselikas L, Deas O, Nicotra C, Ngo-Camus M, Frias RL, Solary E, Angevin E, Eggermont A, Olaussen KA, Vassal G, Michiels S, Andre F, Scoazec JY, Massard C, Soria JC, Besse B,

Friboulet L. Feasibility and first reports of the MATCH-R repeated biopsy trial at Gustave Roussy. NPJ Precis Oncol. 2020 Sep 8;4:27.

6. Eisenhauer EA, Therasse P, Bogaerts J, Schwartz LH, Sargent D, Ford R, Dancey J, Arbuck S, Gwyther S, Mooney M, Rubinstein L, Shankar L, Dodd L, Kaplan R, Lacombe D, Verweij J. New response evaluation criteria in solid tumours: revised RECIST guideline (version 1.1). Eur J Cancer. 2009 Jan;45(2):228-47.
7. Michael R. Filbin, Arnav Mehta, Alexis M. Schneider, Kyle R. Kays, Jamey R. Guess, Matteo Gentili, Bánk G. Fenyves, Nicole C. Charland, Anna L.K. Gonye, Irena Gushterova, Hargun K. Khanna, Thomas J. LaSalle, Kendall M. Lavin-Parsons, Brendan M. Lilly, Carl L. Lodenstein, Kasidet Manakongtreecheep, Justin D. Margolin, Brenna N. McKaig, Maricarmen Rojas-Lopez, Brian C. Russo, Nihaarika Sharma, Jessica Tantivit, Molly F. Thomas, Robert E. Gerszten, Graham S. Heimberg, Paul J. Hoover, David J. Lieb, Brian Lin, Debby Ngo, Karin Pelka, Miguel Reyes, Christopher S. Smillie, Avinash Waghray, Thomas E. Wood, Amanda S. Zajac, Lori L. Jennings, Ida Grundberg, Roby P. Bhattacharyya, Blair Alden Parry, Alexandra-Chloé Villani, Moshe Sade-Feldman, Nir Hacohen, Marcia B. Goldberg. Plasma proteomics reveals tissue-specific cell death and mediators of cell-cell interactions in severe COVID-19 patients. bioRxiv 2020.11.02.365536; doi: https://doi.org/10.1101/2020.11.02.365536
8. Assarsson E, Lundberg M, Holmquist G, Björkesten J, Thorsen SB, Ekman D, Eriksson A, Rennel Dickens E, Ohlsson S, Edfeldt G, Andersson AC, Lindstedt P, Stenvang J, Gullberg M, Fredriksson S. Homogenous 96-plex PEA

immunoassay exhibiting high sensitivity, specificity, and excellent scalability. PLoS One. 2014 Apr 22;9(4):e95192.

9. Vanhersecke L, Brunet M, Guégan JP, Rey C, Bougouin A, Cousin S, Le Moulec S, Besse B, Loriot Y, Larroquette M, Soubeyran I, Toulmonde M, Roubaud G, Pernot S, Cabart M, Chomy F, Lefevre C, Bourcier K, Kind M, Giglioli I, Sautès-Fridman C, Velasco V, Courgeon F, Oflazoglu E, Savina A, Marabelle A, Soria JC, Bellera C, Sofeu C, Bessede A, Fridman WH, Le Loarer F, Italiano A. Mature tertiary lymphoid structures predicts immune checkpoint inhibitor efficacy in solid tumors independently of PD-L1 expression. Nat Cancer 2021, In Press
10. Vigliar E, Malapelle U, Iaccarino A, Acanfora G, Pisapia P, Clery E, De Luca C, Bellevicine C, Troncone G. PD-L1 expression on routine samples of non-small cell lung cancer: results and critical issues from a 1-year experience of a centralised laboratory. J Clin Pathol. 2019; 72:412-417
11. Massard C, Michiels S, Ferté C, Le Deley MC, Lacroix L, Hollebecque A, Verlingue L, Ileana E, Rosellini S, Ammari S, Ngo-Camus M, Bahleda R, Gazzah A, Varga A, Postel-Vinay S, Loriot Y, Even C, Breuskin I, Auger N, Job B, De Baere T, Deschamps F, Vielh P, Scoazec JY, Lazar V, Richon C, Ribrag V, Deutsch E, Angevin E, Vassal G, Eggermont A, André F, Soria JC. High-Throughput Genomics and Clinical Outcome in Hard-to-Treat Advanced Cancers: Results of the MOSCATO 01 Trial. Cancer Discov. 2017 Jun;7(6):586-595.
12. Liao Y, Smyth GK, Shi W. The R package Rsubread is easier, faster, cheaper and better for alignment and quantification of RNA sequencing reads. Nucleic Acids Res. 2019 May 7;47(8):e47.

13. Jiménez-Sánchez A, Cast O, Miller ML. Comprehensive Benchmarking and Integration of Tumor Microenvironment Cell Estimation Methods. Cancer Res. 2019 Dec 15;79(24):6238-6246.
14. Newman AM, Liu CL, Green MR, Gentles AJ, Feng W, Xu Y, Hoang CD, Diehn M, Alizadeh AA. Robust enumeration of cell subsets from tissue expression profiles. Nat Methods. 2015 May;12(5):453-7.
15. Bindea G, Mlecnik B, Tosolini M, Kirilovsky A, Waldner M, Obenauf AC, Angell H, Fredriksen T, Lafontaine L, Berger A, Bruneval P, Fridman WH, Becker C, Pagès F, Speicher MR, Trajanoski Z, Galon J. Spatiotemporal dynamics of intratumoral immune cells reveal the immune landscape in human cancer. Immunity. 2013 Oct 17;39(4):782-95.
16. Keegan A, Ricciuti B, Garden P, Cohen L, Nishihara R, Adeni A, Paweletz C, Supplee J, Jänne PA, Severgnini M, Awad MM, Walt DR. Plasma IL-6 changes correlate to PD-1 inhibitor responses in NSCLC. J Immunother Cancer. 2020 Oct;8(2):e000678.
17. Schalper KA, Carleton M, Zhou M, Chen T, Feng Y, Huang SP, Walsh AM, Baxi V, Pandya D, Baradet T, Locke D, Wu Q, Reilly TP, Phillips P, Nagineni V, Gianino N, Gu J, Zhao H, Perez-Gracia JL, Sanmamed MF, Melero I. Elevated serum interleukin-8 is associated with enhanced intratumor neutrophils and reduced clinical benefit of immune-checkpoint inhibitors. Nat Med. 2020 May;26(5):688-692.
18. Sautès-Fridman C, Petitprez F, Calderaro J, Fridman WH. Tertiary lymphoid structures in the era of cancer immunotherapy. Nat Rev Cancer. 2019;19:307-325.

19. Zhong W, Edfors F, Gummesson A, Bergström G, Fagerberg L, Uhlén M. Next generation plasma proteome profiling to monitor health and disease. Nat Commun. 2021 May 3;12(1):2493.
20. Zhang C, Liu J, Wang J, Hu W, Feng Z. The emerging role of leukemia inhibitory factor in cancer and therapy. Pharmacol Ther. 2020 Nov 28:107754.
21. Gao W, Thompson L, Zhou Q, Putheti P, Fahmy TM, Strom TB, Metcalfe SM. Treg versus Th17 lymphocyte lineages are cross-regulated by LIF versus IL-6. Cell Cycle. 2009 May 1;8(9):1444-50.
22. Duluc D, Delneste Y, Tan F, Moles MP, Grimaud L, Lenoir J, Preisser L, Anegon I, Catala L, Ifrah N, Descamps P, Gamelin E, Gascan H, Hebbar M, and Jeannin P. Tumor-associated leukemia inhibitory factor and IL-6 skew monocyte differentiation into tumor-associated macrophage-like cells. Blood 2007; 110: 4319–4330.
23. Won H, Moreira D, Gao C, Duttagupta P, Zhao X, Manuel E, Diamond D, Yuan YC, Liu Z, Jones J, D'Apuzzo M, Pal S, and Kortylewski M. TLR9 expression and secretion of LIF by prostate cancer cells stimulates accumulation and activity of polymorphonuclear MDSCs. J Leukoc Biol 2017; 102: 423–436.
24. Yaftiyan A, Eskandarian M, Jahangiri AH, Kazemi Sefat NA, Moazzeni SM. Leukemia inhibitory factor (LIF) modulates the development of dendritic cells in a dual manner. Immunopharmacol Immunotoxicol. 2019 Jun;41(3):455-462.
25. Ghanei Z, Mehri N, Jamshidizad A, Joupari MD, Shamsara M. Immunization against leukemia inhibitory factor and its receptor suppresses tumor formation of breast cancer initiating cells in BALB/c mouse. Sci Rep. 2020 Jul 10;10(1):11465.

26. Pascual-García M, Bonfill-Teixidor E, Planas-Rigol E, Rubio-Perez C, Iurlaro R, Arias A, Cuartas I, Sala-Hojman A, Escudero L, Martínez-Ricarte F, Huber-Ruano I, Nuciforo P, Pedrosa L, Marques C, Braña I, Garralda E, Vieito M, Squatrito M, Pineda E, Graus F, Espejo C, Sahuquillo J, Tabernero J, Seoane J. LIF regulates CXCL9 in tumor-associated macrophages and prevents CD8+ T cell tumor-infiltration impairing anti-PD1 therapy. Nat Commun. 2019 Jun 11;10(1):2416. doi: 10.1038/s41467-019-10369-9.

27. Sautès-Fridman C, Petitprez F, Calderaro J, Fridman WH. Tertiary lymphoid structures in the era of cancer immunotherapy. Nat Rev Cancer. 2019;19(6):307-325.

28. Ladányi A, Kiss J, Mohos A, Somlai B, Liszkay G, Gilde K, Fejös Z, Gaudi I, Dobos J, Tímár J. Prognostic impact of B-cell density in cutaneous melanoma. Cancer Immunol Immunother. 2011 Dec;60(12):1729-38.4

29. Messina JL, Fenstermacher DA, Eschrich S, Qu X, Berglund AE, Lloyd MC, Schell MJ, Sondak VK, Weber JS, Mulé JJ. 12-Chemokine gene signature identifies lymph node-like structures in melanoma: potential for patient selection for immunotherapy? Sci Rep. 2012;2:765.

30. Goc J, Germain C, Vo-Bourgais TK, Lupo A, Klein C, Knockaert S, de Chaisemartin L, Ouakrim H, Becht E, Alifano M, Validire P, Remark R, Hammond SA, Cremer I, Damotte D, Fridman WH, Sautès-Fridman C, Dieu-Nosjean MC. Dendritic cells in tumor-associated tertiary lymphoid structures signal a Th1 cytotoxic immune contexture and license the positive prognostic value of infiltrating CD8+ T cells. Cancer Res. 2014 Feb 1;74(3):705-15.

31. Behr DS, Peitsch WK, Hametner C, et al. (2014) Prognostic value of immune cell infiltration, tertiary lymphoid structures and PD-L1 expression in Merkel cell carcinomas. Int J Clin Exp Pathol 7:7610–7621.
32. Caro GD, Bergomas F, Grizzi F, et al. (2014) Occurrence of tertiary lymphoid tissue is associated with T-cell infiltration and predicts better prognosis in early-stage colorectal cancers. Clin Cancer Res 20:2147–2158.
33. Schram A, Borazanci E, Brana I, Vieito Villar M, Garralda E, Spreafico A, Oliva M, Lakhani N, Wasserman R, Hoffmann K, Hallett R, Anido J, Maetzel D, Giblin P, Moran E, Kelly A, Seoane J, Von Hoff D, Siu L, Tabernero J. Phase 1 dose escalation of MSC-1, a humanized anti-LIF monoclonal antibody, in patients with advanced solid tumors [abstract]. In: Proceedings of the Annual Meeting of the American Association for Cancer Research 2020; 2020 Apr 27-28 and Jun 22-24. Philadelphia (PA): AACR; Cancer Res 2020;80(16 Suppl):Abstract nr CT147.

FIGURES LEGENDS

Figure 1. Flow chart depicting the identification strategy of a biomarker associated to resistance to anti-PD(L)1 immunotherapy within a discovery cohort and its assessment in an additional validation cohort. Pre-treatment (Pre-Tx) plasma samples and matched tumor biopsies were collected before anti-PD1/PDL1 antibodies-based treatment in cancer patients (see Table 1 for patient details). Plasma samples (n=95 patients) were processed for a comprehensive proteomic analysis allowing the simultaneous detection of 1463 proteins. Tumor biopsies were exploited for **i)** RNA-Sequencing for tumor immune gene expression profile (n=52 patients) and for **ii)** immunohistochemistry in order to assess tumor PDL1 expression (TPS score), CD8 T-cells density and the presence of Tertiary Lymphoid Structures (TLS) (n=59 patients). Computed data were then tested for their association with clinical data including clinical outcome. Durable Clinical Benefit (DCB) was considered for patients deriving complete or partial response but also a stable disease with a progression free survival (PFS) > 12months. Non Durable Benefit (NDB) was considered for patients with a progressive disease or a stable disease with a PFS ≤ 12 months. The best selected biomarker was investigated in an independent validation cohort of 292 patients (see Table 1 for patients' details) receiving PD1 / PDL1 blockade antibodies.

Figure 2. Baseline plasmatic LIF level predicts response to PD1 / PDL1 axis blockade. A Display of the Log Rank p-values for progression-free survival (PFS) (y axis) and of the delta median PFS (y axis) associated with each plasmatic marker. Median value of each plasmatic marker was used to categorize patients with High or Low status. Each dot represents one marker. **B** Kaplan Meier curves of progression-free survival (left) and overall survival (right) according to baseline plasmatic LIF levels. **C** Quantification of baseline plasmatic LIF in NDB (n= 72, blue) and DCB (n= 23, red) patients. p value was calculated using Wilcoxon Rank sum test. **D** Proportion of patients who experienced durable clinical benefit (DCB) or non-clinical benefit (NCB) according to their baseline plasmatic level of LIF classified as High (above median value) and Low (below median value).

Figure 3. LIF is a predictive biomarker independently from PDL1 expression status and tumoral CD8 infiltration level. A PDL1 expression was assessed by immunohistochemistry (PDL1 stained in purple). Illustrations here depict tumor cases with negative (TPS<1%) and positive (TPS ≥ 1%) PDL1 expression. **B** Representation of plasmatic LIF level in patients according to their PDL1 TPS score (TPS<1 vs TPS ≥1). p value was calculated using Wilcoxon Rank sum test. **C** PFS probability according to LIF level (High vs Low) in patients negative (TPS<1, n=39) or positive (TP≥1, n=20) for tumoral PDL1 expression. **D** CD8+ T cell infiltration was assessed through immunohistochemistry staining (CD8 stained in brown). Illustrations highlight tumor cases with low and high CD8 infiltration level. E Plasmatic LIF level in patients according to their CD8 infiltration level. p value was calculated using Wilcoxon Rank sum test. **E** PFS probability according to LIF level (High vs Low) in patients classified as $CD8^{Low}$ (n=44) or $CD8^{High}$ (n=15).

Figure 4. Peripheral LIF level is associated with an intratumoral B cell signature and presence of Tertiary Lymphoid Structures. A Correlation of immune cell lineages - obtained through RNA-sequencing and data deconvolution with Bindea algorithm - and LIF plasma level. Dot size depicts the correlation coefficient while the color is indicative of positive (red) or negative (blue) correlation. The X-axis represents the transformed Log10 pearson p-value. **B** Histogram representation of B cell score (in relative units, RU) according to baseline plasmatic level of LIF classified as High or Low (median value used as a cut-off). p value was calculated using a Wilcoxon Rank sum test. **C** Representative histological images from a patient with squamous cell lung carcinoma showing presence of TLS highlighted through both Hematoxylin Eosin Saffron (HES) staining and double staining of CD3-CD20 (CD3 in brown, CD20 in purple). Left image has been captured at a low magnification – scale bar indicates 400µm size – while the images on the right has been obtained through slide digitization at a higher magnification; scale bar indicates 100µm. Black arrow indicates tumor cells that juxtapose TLS. **D** Proportion of patients with presence or absence of intratumoral TLS according to baseline LIF plasma level. p value was calculated through Chi-squared test.

Figure 5. Baseline circulating LIF level is predictive of outcome of cancer patients treated with anti-PD(L)1 immunotherapy – results from an independent validation cohort. A Probability of PFS for LIF ^{High} (median survival = 2,57 mo.) and LIF ^{Low} (median survival = 5,07 mo.) patients in the Validation Cohort (n = 292). **B** Probability of OS for LIF ^{High} (median survival = 8,53 mo.) and LIF ^{Low} (median survival = NA) patients in the same patients cohort. **C** Proportion of patients who experienced DCB or NCB according to their baseline plasmatic level of LIF classified as High (above median value) and Low (below median value). P value was calculated through Chi-squared test.

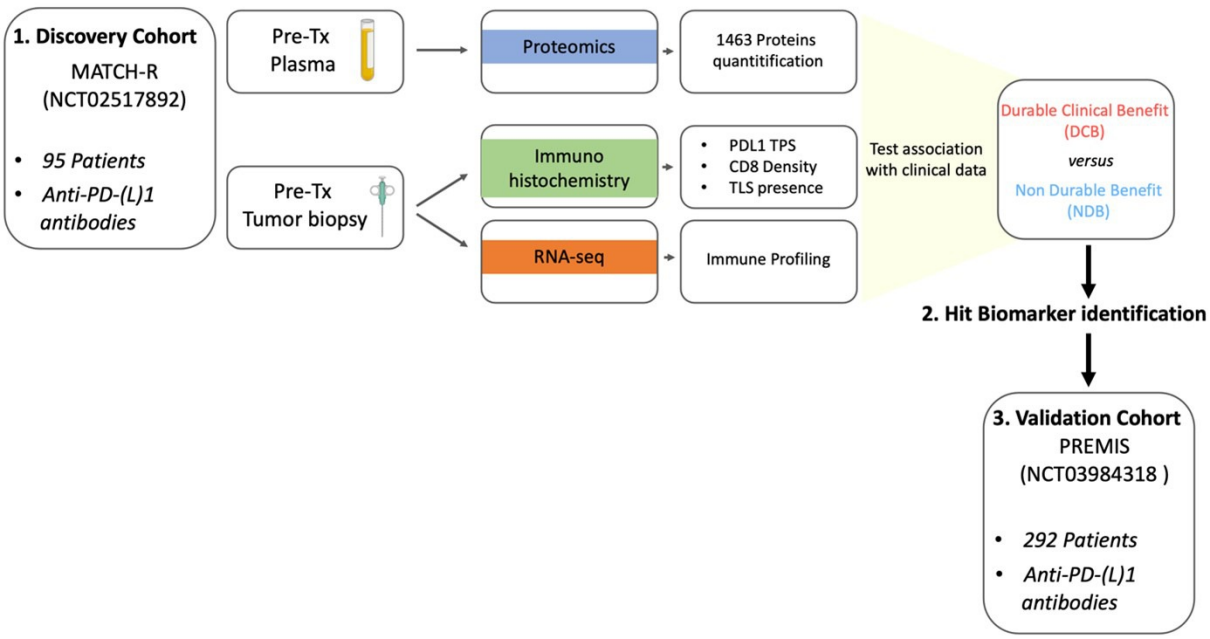
1. Discovery Cohort
MATCH-R
(NCT02517892)
95 Patients
Anti-PD-(L)1 antibodies
Pre-Tx Plasma
Pre-Tx Tumor biopsy
Proteomics
Immuno histochemistry
RNA-seq
1463 Proteins quantitification
PDL1 TPS
CD8 Density
TLS presence
Immune Profiling
Test association with clinical data
Durable Clinical Benefit (DCB)
versus
Non Durable Benefit (NDB)
2. Hit Biomarker identification
3. Validation Cohort
PREMIS
(NCT03984318)
292 Patients
Anti-PD-(L)1 antibodies

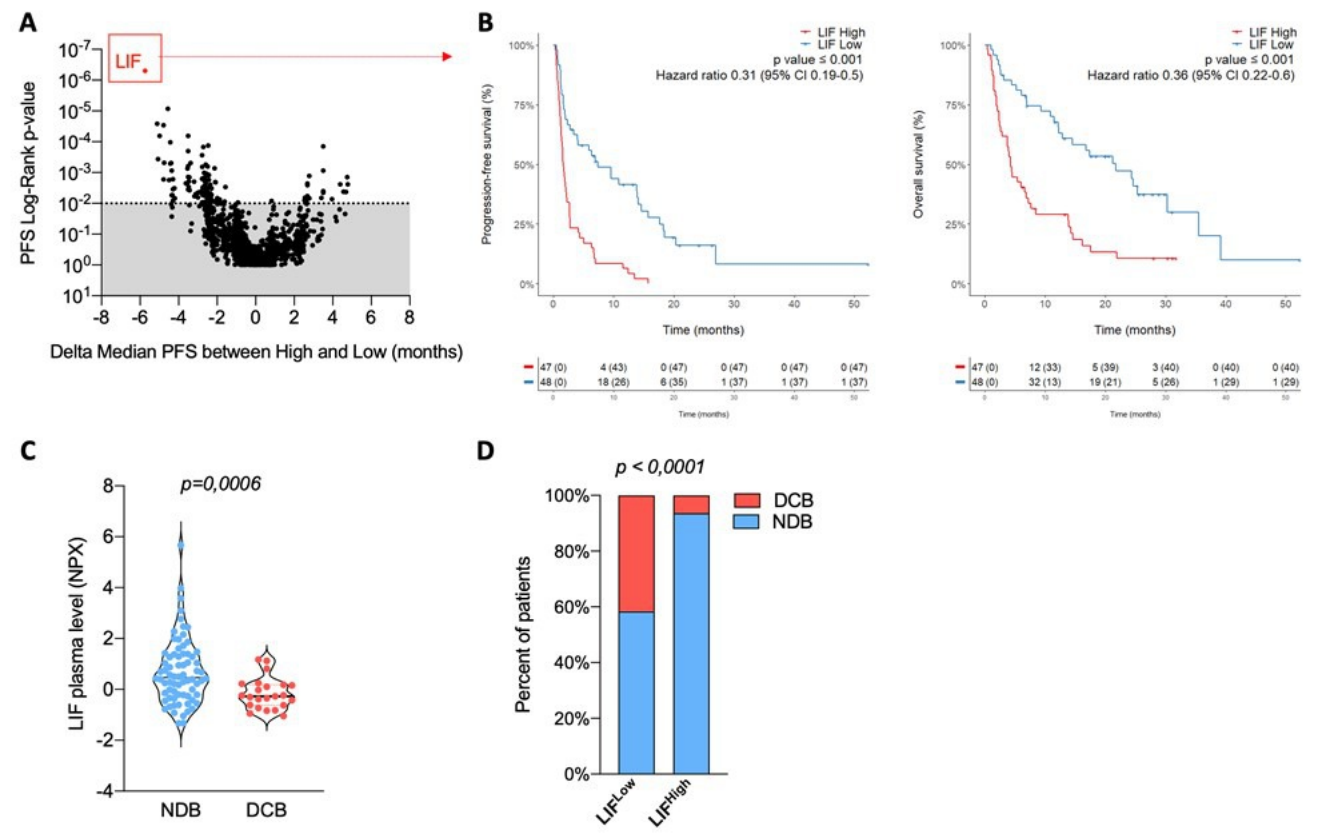
A
LIF
PFS Log-Rank p-value
Delta Median PFS between High and Low (months)
B
LIF High
LIF Low
p value ≤ 0.001
Hazard ratio 0.31 (95% CI 0.19-0.5)
Progression-free survival (%)
Time (months)
47 (0) 4 (43) 0 (47) 0 (47) 0 (47) 0 (47)
48 (0) 18 (26) 6 (35) 1 (37) 1 (37) 1 (37)
Hazard ratio 0.36 (95% CI 0.22-0.6)
Overall survival (%)
47 (0) 12 (33) 5 (39) 3 (40) 0 (40) 0 (40)
48 (0) 32 (13) 19 (21) 5 (26) 1 (29) 1 (29)
C
p=0,0006
LIF plasma level (NPX)
NDB
DCB
D
p < 0,0001
DCB
NDB
Percent of patients
LIFLow
LIFHigh

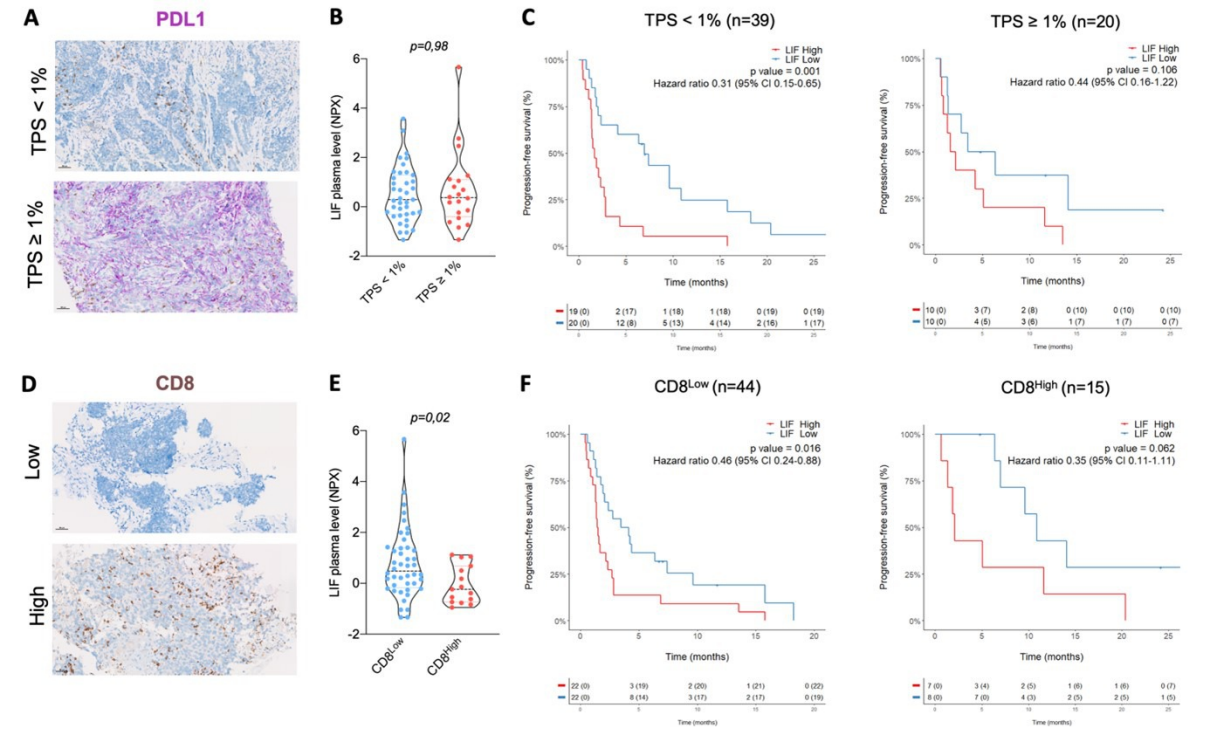
A
PDL1
TPS < 1%
TPS ≥ 1%
B
p=0,98
LIF plasma level (NPX)
TPS < 1%
TPS ≥ 1%
C
TPS < 1% (n=39)
LIF High
LIF Low
p value = 0.001
Hazard ratio 0.31 (95% CI 0.15-0.65)
Progression-free survival (%)
Time (months)
19 (0) 2 (17) 1 (18) 1 (18) 0 (19) 0 (19)
20 (0) 12 (8) 5 (13) 4 (14) 2 (16) 1 (17)
TPS ≥ 1% (n=20)
LIF High
LIF Low
p value = 0.106
Hazard ratio 0.44 (95% CI 0.16-1.22)
Progression-free survival (%)
Time (months)
10 (0) 3 (7) 2 (8) 0 (10) 0 (10) 0 (10)
10 (0) 4 (5) 3 (6) 1 (7) 1 (7) 0 (7)
D
CD8
Low
High
E
p=0,02
LIF plasma level (NPX)
CD8Low
CD8High
F
CD8Low (n=44)
LIF High
LIF Low
p value = 0.016
Hazard ratio 0.46 (95% CI 0.24-0.88)
Progression-free survival (%)
Time (months)
22 (0) 3 (19) 2 (20) 1 (21) 0 (22)
22 (0) 8 (14) 3 (17) 2 (17) 0 (19)
CD8High (n=15)
LIF High
LIF Low
p value = 0.062
Hazard ratio 0.35 (95% CI 0.11-1.11)
Progression-free survival (%)
Time (months)
7 (0) 3 (4) 2 (5) 1 (6) 1 (6) 0 (7)
8 (0) 7 (0) 4 (3) 2 (5) 2 (5) 1 (5)

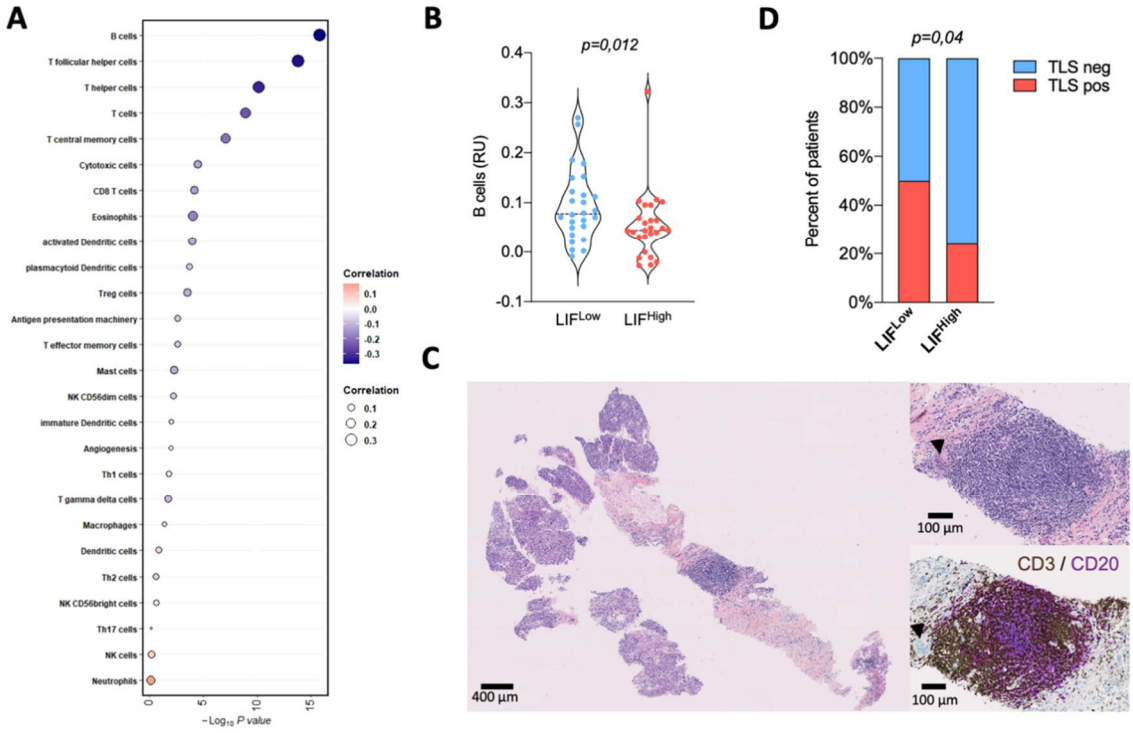

Figure 4. Peripheral LIF level is associated with an intratumoral B cell signature and presence of Tertiary Lymphoid Structures. A Correlation of immune cell lineages - obtained through RNA-sequencing and data deconvolution with Bindea algorithm - and LIF plasma level. Dot size depicts the correlation coefficient while the color is indicative of positive (red) or negative (blue) correlation. The X-axis represents the transformed Log10 pearson p-value. **B** Histogram representation of B cell score (in relative units, RU) according to baseline plasmatic level of LIF classified as High or Low (median value used as a cut-off). p value was calculated using a Wilcoxon Rank sum test. **C** Representative histological images from a patient with squamous cell lung carcinoma showing presence of TLS highlighted through both Hematoxylin Eosin Saffron (HES) staining and double staining of CD3-CD20 (CD3 in brown, CD20 in purple). Left image has been captured at a low magnification – scale bar indicates 400µm size – while the images on the right has been obtained through slide digitization at a higher magnification; scale bar indicates 100µm. Black arrow indicates tumor cells that juxtapose TLS. **D** Proportion of patients with presence or absence of intratumoral TLS according to baseline LIF plasma level. p value was calculated through Chi-squared test.

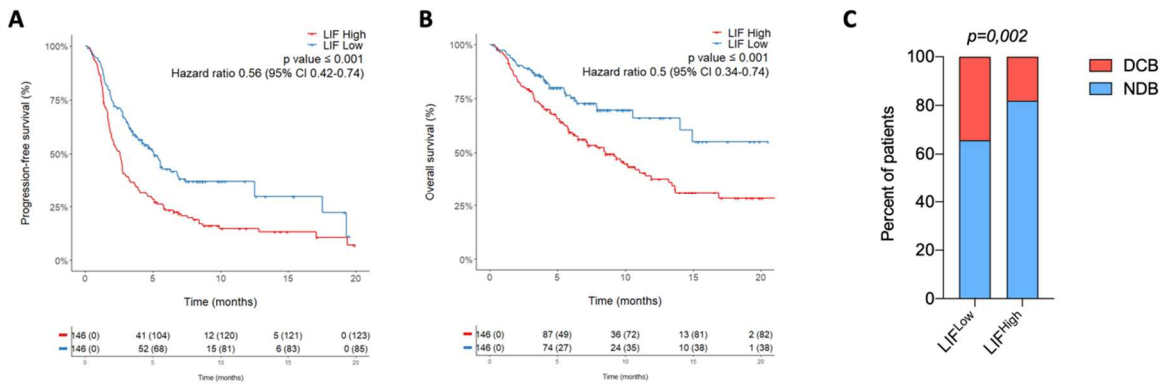

Figure 5. Baseline circulating LIF level is predictive of outcome of cancer patients treated with anti-PD(L)1 immunotherapy – results from an independent validation cohort. A Probability of PFS for LIF ^{High} (median survival = 2,57 mo.) and LIF ^{Low} (median survival = 5,07 mo.) patients in the Validation Cohort (n = 292). **B** Probability of OS for LIF ^{High} (median survival = 8,53 mo.) and LIF ^{Low} (median survival = NA) patients in the same patients cohort. **C** Proportion of patients who experienced DCB or NCB according to their baseline plasmatic level of LIF classified as High (above median value) and Low (below median value). P value was calculated through Chi-squared test.

TABLE 1. Patient characteristics		
Discovery cohort (n=95)		
Age	Median 63 years (range 34-91)	
Gender	N	%
Male	61	64.2
Female	34	35.8
Tumor Type		
Non-small cell lung cancer	71	74.7
Bladder cancer	13	13.7
Others[1]	11	11.6
Performance status		
≤ 1	78	82.1
> 1	17	17.9
Stage IV cancer	95	100
Treatment		
Anti-PD1	66	69.5
Anti-PD-L1	22	23.1
PD1 or anti-PD-L1 + another immunecheckpoint	7	7.4
Validation Cohort (n=292)		
Age	Median 61 years (range 25-97)	
Gender	N	%
Male	173	59.2
Female	119	40.8
Tumor Type		
Non-small cell lung cancer	107	36.6
Melanoma	24	8.2

Soft-tissue sarcoma	22	7.5
Kidney	19	6.5
Bladder	15	5.1
Others[2]	105	36.0
Performance status		
≤ 1	244	83.6
> 1	48	16.4
Previous lines of treatment		
≤ 1	100	34.2
> 1	192	65.8
Treatment		
Anti-PD1	160	54.8
Anti-PD-L1	101	34.6
Combination of Immune Checkpoint	31	10.6

[1]prostate carcinoma, biliary tract cancer, thyroid cancer, prostate carcinoma, uterine carcinoma, [2]cervix carcinoma, colorectal cancer, gastric cancer, head and neck cancer, renal cancer, soft-tissue sarcoma, triple negative breast carcinoma

TABLE 2. Multivariate Analysis for Progression-Free Survival and Overall Survival			
Progression-Free Survival			
Independent Variables		Hazard ratio	P value
ECOG CODE	≤1	0.43 95% CI [0.29-0.65]	<0.001
	≥2	1	
Liver metastasis	Yes	1	0.042
	No	0.67 95% CI [0.46-0.98]	
Number_of_previous lines of treatment	≤1	0.61 95% CI [0.44-0.86]	0.004
	≥2	1	
LIF plasma levels	High	1.51 95% CI [1.1-2.1]	0.013
	Low	1	
Overall Survival			
	B	Hazard ratio	P value
ECOG CODE	≤1	0.21 95% CI [0.13-0.35]	<0.001
	≥2	1	
Liver metastasis	Yes	1	0.008
	No	0.54 95% CI [0.34-0.85]	
Number_of_previous lines of treatment	≤1	0.61 95% CI [0.40-0.94]	0.027
	≥2	1	
LIF plasma levels	High	1.78 95% CI [1.14-2.77]	0.01
	Low	1	